4. Experimental testing of a magnetic shield type superconducting fault current limiter

Introduction

In this chapter the experimental activity carried out on a prototype of magnetic shield type fault current limiter at the Laboratory of Applied Superconductivity of the University of Bologna is described. The aim of this activity is to collect an extensive set of data for the wide range validation of the numerical model presented in the previous chapters, also with reference to the future developments needed to take account of the effect of the temperature.

In section 4.1 an 4.2 the prototype and the test circuit are described. In section 4.3 the results of the short circuit tests performed are reported. In section 4.4 an equivalent circuit of the device is derived and the experimental and numerical waveforms are compared.

4.1 The fault current limiter prototype

The equivalent circuit of a magnetic shield type superconducting fault current limiter presented in section 3.4 is validated through the comparison of the numerical results with the experimental data available in the technical literature, which refer to specific operating conditions. However, in order to carry out a complete inspection of the applicability of the model, a larger amount of experimental results is needed. In this section we describe the fault current limiter prototype that has been designed and manufactured at the Laboratory of Applied Superconductivity of the University of Bologna [84]. The aim of this device is to collect an extensive set of data for the wide range validation of the numerical model, particularly with reference to the extension needed to take account of the effect of the temperature. Before seeing the details of the prototype, let us have a look to some general considerations concerning this kind of device.

A magnetic shield type superconducting fault current limiter consists of a normal coil and a superconducting tube coupled inductively via a ferromagnetic core, as shown schematically in figure 3.4.1. The normal coil is series connected with the protected circuit.

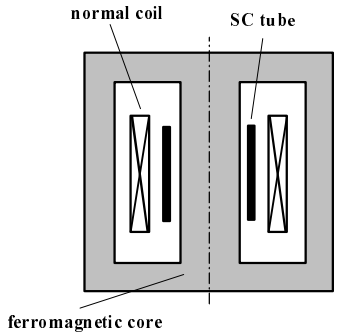

Figure 3.4.1: scheme of a magnetic shied type SFCL

The function of the device is the change of its impedance from a low (ideally zero) to an high value, which depends on the parameters of the protected circuit, when the current exceeds some "quenching" value I_q. This rise of impedance produces the

limiting effect. Let us indicate with “non-limiting state” the condition in which the tube is in the superconducting state, and with “limiting state” the condition in which the superconducting/normal transition of the tube is complete; moreover, let us denote with Z_{NL} and Z_L the impedance of the device during the non-limiting an the limiting state respectively. Due to leakage fluxes, the non-limiting impedance of an actual device has a non zero complex part. Moreover due to joule heating in the normal coil, losses in the ferromagnetic core and AC losses in the SC tube, also the real part of Z_{NL} is non zero. As long as the current of the protected circuit remains below $I_{q,}$ the shielding currents induced in the tube do not overcome the critical value and the tube maintains the superconducting state. In this condition the heat produced by AC losses is removed by the coolant. In case of a fault the circuit current grows beyond $I_{q,}$ therefore the SC tube enters the transition toward a normal state and both the losses inside the tube and the penetration of the magnetic field in the core rise thus causing an increase of the resistance and the inductance (in a word the impedance, even though we are not strictly speaking of steady sinusoidal regime); however, the increase of the inductance is dominant, that’s why this device is referred to as *inductive*. At this point the thermal equilibrium is broken and the overheating produces a rise of the temperature; a series connected circuit breaker open the circuit in order to avoid damages to the ring. After the fault is removed the breaker re-closes the circuit and at this moment the tube must have fully restored the superconducting state. The minimum time interval allowing the recovering of the tube is the “recovery time” t_r. The quenching current I_q, the non-limiting and the limiting impedance Z_{NL} and Z_L, and the recovery time t_r are the main design parameters of a superconducting fault current limiter.

Let us now consider the design of the prototype; in order to define its final layout we proceed as follows: first we choose the superconducting element, then we define the normal conducting coil and finally we specify the ferromagnetic core on the base of the assumed design parameters.

- the superconducting tube

We choose as superconducting element a commercial available BiSCCO 2212 tube manufactured by Nexans. The dimensions and the critical current density are reported in figure 4.1.1, together with the experimental E-J characteristic supplied by the manufacturer.

Inner diameter:	103 *mm*
Outer diameter	113 *mm*
Height	50 *mm*
Critical current density J_c [1 $\mu V/cm$, 77 *K, self field*]	810 A/cm^2
Critical current I_c [1 $\mu V/cm$, 77 *K, self field*]	2025 A

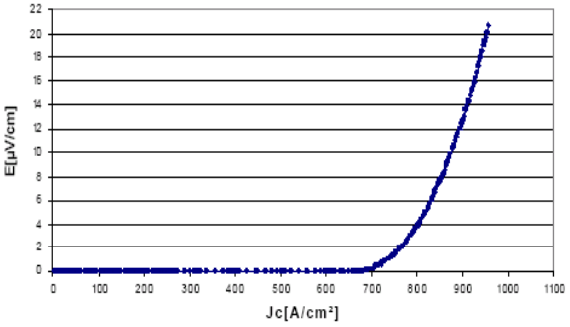

Figure 4.1.1: E-J characteristic of the BiSCCO 2212 tube

The experimental E-J characteristic is well fitted by the power law with the n exponent equal to 10. This choice of the SC tube imposes some geometrical constrains on the inner diameter of the normal coil and the diameter of the ferromagnetic core column.

- the normal conducting coil

The normal coil consists of 285 turns, arranged in 15 layers of 19 turns each and made by using a 2 × 5 mm^2 copper tape. The inner diameter of the coil is equal to 160 mm. A paper insulating sheet is placed between the layers. The thickness and height of the coil are equal to 43 and 104 mm respectively. The maximum magneto-motive force which can be shielded by the chosen SC tube with an acceptable level of losses is equal to its critical current, i.e. 2025 A. In case of perfect magnetic coupling the total current circulating in the SC tube is equal (and opposite) to the magneto-motive force produced by the coil. The quenching current I_q of the device is conventionally defined as the current of the normal coil which induces in the SC tube a total current equal to the critical one. With the above layout of the coil the device quenching current I_q results equal to about 7 A. However, due to non perfect magnetic coupling the actual transition of the device to an high impedance state is expected to be detected for an higher value of current.

- the ferromagnetic core

For what concern the magnetic core, a column with circular cross section of 63 mm diameter, made of laminated grain oriented silicon steel, is chosen. With this open core configuration the ratio between the limiting and the non–limiting state impedance of the device is too small to be of practical interest; however, with a proper choose of the column height, the Z_{NL}/Z_L ratio can be large enough to affect current and voltage waveforms in a way detectable by the instrumentation of the laboratory [14,85]. Figure 4.1.2 shows the calculated value of the ratio Z_{NL}/Z_L as a function of the height of the column.

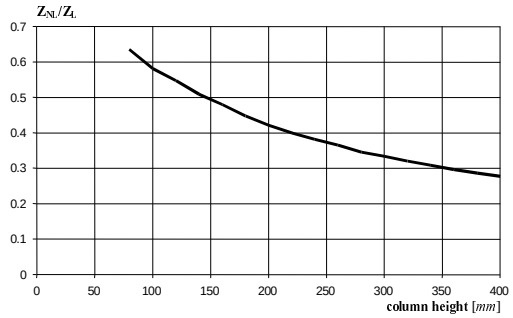

Figure 4.1.2: impedence ratio of the open core magnetic shied type SFCL

By choosing a column height of 300 *mm* we obtain value of the ratio Z_{NL}/Z_L equal to 1/3. The calculated values of Z_{NL} and Z_L are respectively 3.89 and 11.26. Such a ratio allows the device to produce a significant limiting effect in case of a fault. The final layout of the prototype is shown in figure 4.1.3. The dimension are expressed in *mm*.

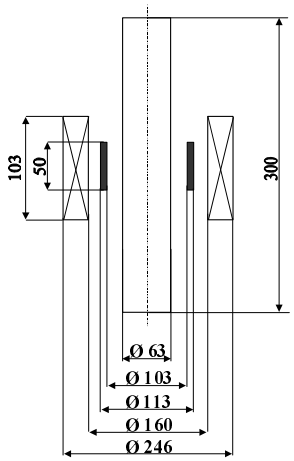

Figure 4.1.3: layout of the prototype

4.2 The experimental set up

The test circuit for the device is represented in figure 4.2.1. The FCL prototype is series connected to a protective resistance R_P of 1 Ω and to a load resistance R_L of 9 Ω. The circuit is supplied by an autotransformer connected to the 220V/50Hz AC network and is controlled by a means of a triac SW_1. The load resistance is parallel connected to a second triac SW_2 which command the fault.

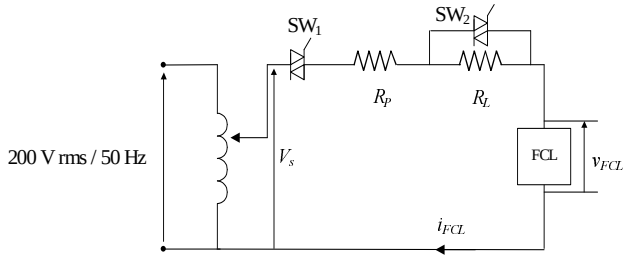

figure 4.2.1. test circuit.

The voltage V_s of the source, the voltage V_{FCL} across the device and the current I_{FCL} flowing in the circuit are acquired by means of insulated Hall effect transducers, connected to a multi-channel data acquisition card (ni 6024), with a sampling rate of 750 samples per second. Two digital I/O channels of the card have been used to control the insulated drivers of the triacs. The system is managed by means of the LabVIEW software. During the tests the whole device is immersed in a liquid nitrogen bath.

The short circuit tests are performed according to the following procedure: first both the driving signals of triacs SW_1 and SW_2 are set to zero. The voltage of the autotransformer is adjusted to the desired value. The driving signal of triac SW_1 is switched on at a time conventionally assumed equal to zero; at this point the data acquisition starts. The circuit works in nominal operating conditions, i.e. the FCL stands in the non limiting state. After a time long enough for the transient component of the current to vanish (the time constant of the circuit is about 1 ms), the driving signal of triac SW_2 is switched on at time t_{fault}, when the circuit current is crossing the zero. Both the triacs SW_1 and SW_2 switch off at t_{end} equal to 220 *ms*. The described switching procedure for a short circuit test is represented in figure 4.2.2.

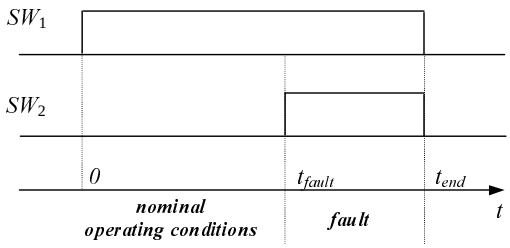

figure 4.2.2. switching sequence

4.3 Experimental results

In order to evaluate the device impedance in the limiting and non-limiting state and to determine the value of the quenching current, a preliminary series of experiments is carried out. The resistance R_L is bypassed by means of the switch SW2 and the SW1 is turned on for 160 ms, a time sufficient for the circuit current to reach the regime course and short enough not to damage the SC element with overheating. The test circuit is supplied with low values of voltage. First the device is tested without the SC ring inserted. In this condition the device impedance, evaluated as the ratio of peaks value of the experimental current and voltage waveforms, both sinusoidal, is found to be equal 10.01 Ω, essentially inductive for a lag angle of π/2 rad is observed between current and voltage. When the SC tube is inserted, the value of the device impedance is found to be equal to 4.37 Ω, confirming the shielding effect. Even in this case the resistive part of the impedance was negligible. By repeating the test with gradually increasing supply voltages, a linear growth of the peak value of circuit current is observed and the low value of the impedance is maintained, until the value of 15 A is reached. By further increasing the supply voltage, some spikes begin to appear in the waveform of the voltage across the device, which is no longer sinusoidal, and a consequent drop in the circuit current peak is observed. This means that, corresponding to the value of current I_q = 15 A, the SC ring enters the SC/normal transition and the prototype begins to switch toward the high impedance state.

The experimental waveforms of current and voltage across the device during a fault test for different values of voltage of the power supply, are shown in the figures 4.3.1 – 4.3.8. The calculated non limited current, i.e. the current which would circulate in the circuit if the FCL stayed always in the non limiting state, is also shown in the figures. As it can be seen from the figures, as long as the circuit is under normal (non fault) operating conditions, the current remains below I_q and the corresponding voltage across the device is sinusoidal and displaced by an angle of π/2 rad; in this phase the FCL behaves like a reactance of 4.37 Ω, confirming what is observed with the preliminary tests. When, due to a fault, the circuit current overcomes the value I_q, a reduction of its first peak respect to the first peak of the non limited current is observed, confirming that the SC tube enters the SC/normal transition and the prototype switches to an higher

impedance state. In order to avoid overheating of the tube the circuit is turned off after few cycles. The extent of the limiting effect, i.e. the difference between the first peak of the non limited and the limited current expressed as a percentage of the non limited one, increases with the increase of the fault severity. The maximum limiting effect recorded is equal to 31%. It must be considered that, for a given test circuit, a magnetic shield type FCL with a closed magnetic core produces a stronger limiting effect. The course of the current peaks and the limiting effect as a function of the voltage of the power supply is shown in figure 4.3.9 (the limiting effect is quoted with respect to the same axis as the current peaks);

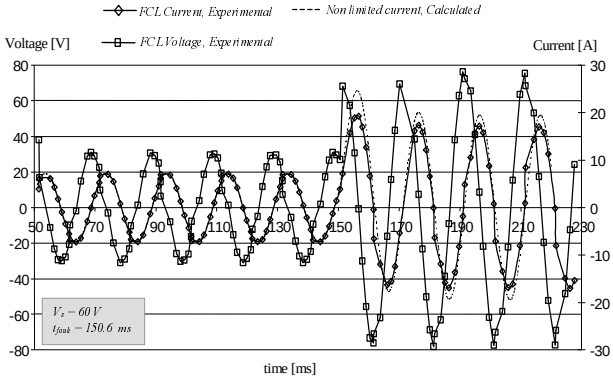

Figure 4.3.1: Current and voltage across the device during a fault. V_s = 60 V rms; t_{fault} = 150.6 ms.

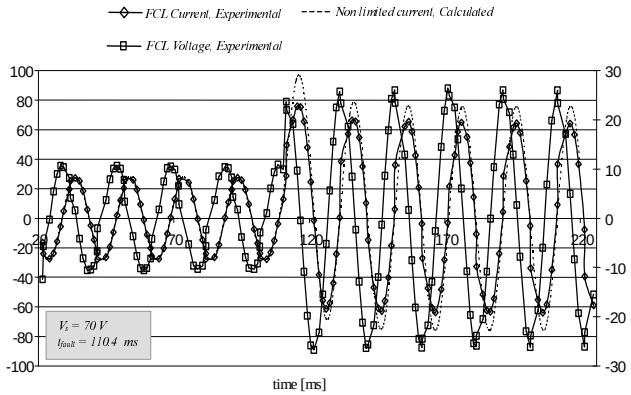

Figure 4.3.2: Current and voltage across the device during a fault. V_s = 70 V rms; t_{fault} = 110.4 ms.

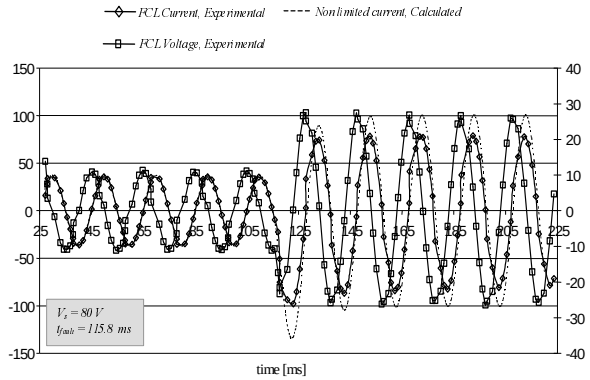

Figure 4.3.3:Current and voltage across the device during a fault. V_s = 80 V rms; t_{fault} = 115.8 ms

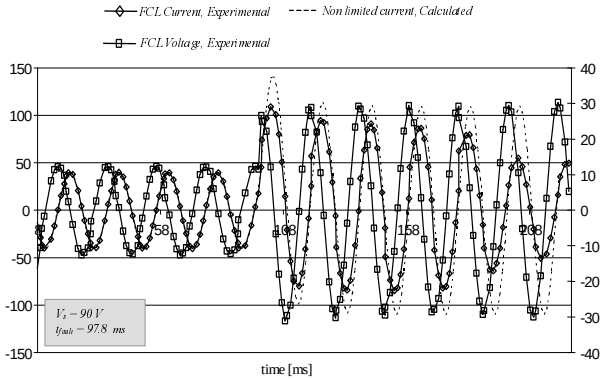

Figure 4.3.4:Current and voltage across the device during a fault. V_s = 90 V rms; t_{fault} = 97.8 ms.

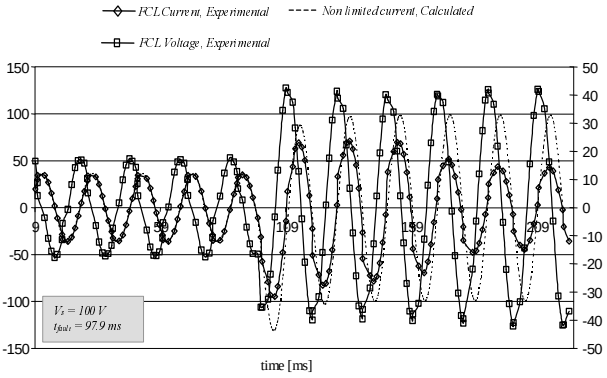

Figure 4.3.5:Current and voltage across the device during a fault. V_s = 100 V rms; t_{fault} = 97.9 ms

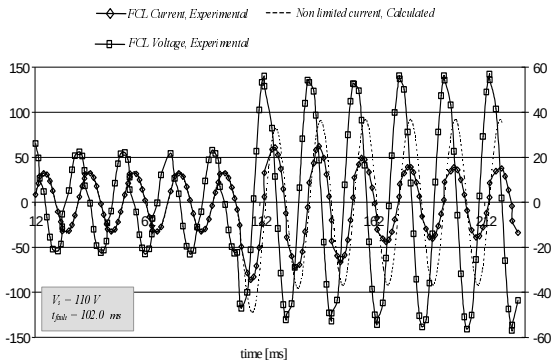

Figure 4.3.6:Current and voltage across the device during a fault. V_s = 110 V rms; t_{fault} = 102.0 ms

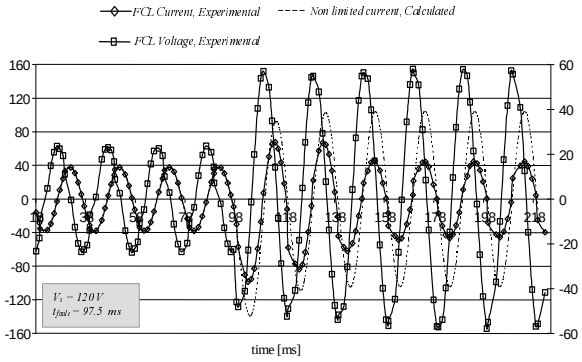

Figure 4.3.7:Current and voltage across the device during a fault. V_s = 120 V rms; t_{fault} = 97.5 ms

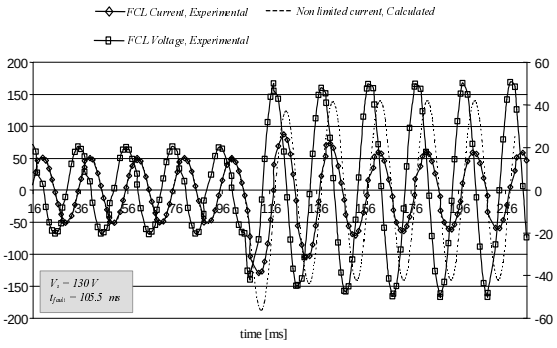

Figure 4.3.8:Current and voltage across the device during a fault. V_s = 130 V rms; t_{fault} = 105.5 ms

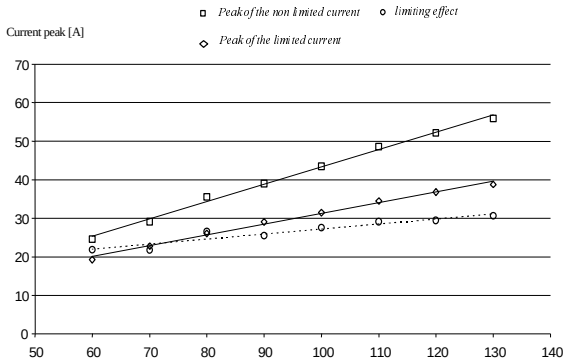

Figure 4.3.9: current peaks and limiting effect

(the limiting effect is quoted with respect to the same axis as the current peaks);

4.4 Numerical results

The model of the equivalent electric and magnetic networks presented in section 3.2-3.3 can be used to determine the equivalent circuit of the magnetic shield type fault current limiter prototype described in section 4.1, following the approach discussed in section 3.4. The equivalent circuit can be easily coupled with the test circuit of section 4.2 and the experimental waveforms of current and voltage shown in section 4.3 can be numerically calculated through it in order to verify its accuracy.

In order to define the equivalent circuit, two meshes, one for the SC tube and one for the ferromagnetic core, are defined. Both the meshes are made of triangular prisms. As discussed in section 3.4, to reproduce accurately the process of current penetration in the SC material a large number of elements is required for the SC mesh; however, when only the voltage across the normal conducting coil of the SCFCL is considered, the difference in the numerical results arising from the details of current distribution, especially in the radial direction, is not significant. Therefore, with reference to the FCL voltage only, the numerical convergence is reached even with coarse meshes of the SC ring. For what concerns the mesh of the ferromagnetic core, the numerical convergence is reached only with a quite fine discretization along the column axis. Simulations with different number of elements both for the SC ring mesh and for the ferromagnetic core mesh have been considered in order to verify the convergence of the numerical solution, however, the numerical results shown below refer to the smallest meshes which are able to reproduce the convergence value of voltage across the SCFCL. The SC ring mesh is the same used in section 3.4 (see page 144); it consists of three rings of 24 prisms with triangular basis each. Each ring is divided in 12 sectors made of two prisms which span the ring thickness. This arrangement of elements allows only one current per layer circulating in the azimuthal direction; no details of current distribution in the radial direction comes out from this discretization. More refined discretization of SC ring in radial and axial directions does not significantly affect the numerical voltage waveform. The results corresponding to lower number of layers are instead significantly different. For the magnetizable core mesh, the circular cross section of the column is divided in 32 triangles. In order to reach the convergence, 26 layers of prisms are needed. Lower number of layers gives results

underestimated and far from convergence. Refinement of this mesh in radial direction does not significantly change the numerical results. Notice that in the present case a fine mesh of the magnetizable core is required, whereas in the case of section 3.4 a coarse mesh was sufficient. The difference is due to the fact that, as discussed in section 2.2. (see pages 86-87), for what concern the magnetizable part, the numerical convergence is very fast if a closed magnetic configuration, as the one dealt with in section 3.4, is considered.

Since the numerical results obtained have shown that no appreciable current flows in the axial direction, the circuit branches connecting neighboring elements which belong to different layers have been eliminated from the equivalent circuit of the device; Branches belonging to different layers are then coupled by means of inductive effects only. Figure 4.4.1 shows the equivalent circuit of the device obtained by the two meshes under this assumption when the iron core is considered linear, connected with the test circuit. The right side of the circuit is the network associated to the SC ring. The linear inductances represent both the auto induction coefficient of the branch current and the mutual induction coefficients with all other currents.

Currents denoted by i_1, i_2, and i_3 are the shielding currents flowing in the three rings of the SC mesh. The non linear resistors $\mathcal{R}_1$, $\mathcal{R}_2$ and $\mathcal{R}_3$ are all defined by the law $U = K(i / i_c)^n sign(i)$, where i_c is the critical current of the SC ring corresponding to the circuit loop (one third of the critical current of the whole SC tube), and n is the exponent of the power law assumed for modeling the SC material. For the numerical simulation the relative magnetic permeability of the iron core is assumed to be equal to 10000. The critical current density of SC tube is assumed to be 810 A/cm^2 and the exponent n of the *E-J* power law is assumed to be equal to 10. The parameters of the SFCL equivalent circuit are reported in Table 4.4.I.

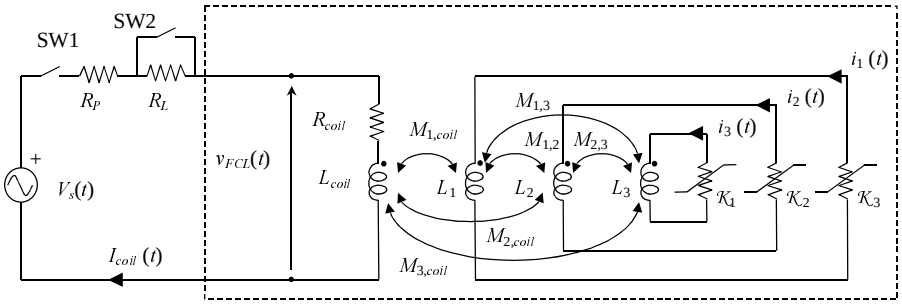

Figure 4.4.1. Equivalent circuit of the FCL prototype.

Table. 4.4.I: parameters of the equivalent circuit of the SFCL prototype

R_{coil}	0.300 Ω
L_{coil}	28.22 mH
$L_1 = L_3$	0.507 μH
L_2	0.510 μH
$M_{1,2} = M_{2,3}$	0.413 μH
$M_{1,3}$	0.354 μH
$M_{1,coil} = M_{3,coil}$	-0.820 μH
$M_{2,coil}$	-0.840 μH
K	100 μV
i_c	692.7 A
n	10

The numerically calculated waveforms of current and voltage across the device during a fault test are shown in figure 4.4.2 and 4.4.3, for two different value of voltage of the power supply, together with the experimental ones. As it can be seen from the figures, as far as the current does not exceeds the trigger value and the device remains in the low impedance state, the numerical results are in a good agreement with the experimental ones; this means that the equivalent circuit well reproduces the shielding effect of the SC ring. Moreover, the current and voltage during a short period after the fault occurrence are also well reproduced. A discrepancy begins to appear after some cycles. The heavier the fault and the losses produced, the more the mismatch becomes remarkable, suggesting that the thermal effect becomes important. The reduction of the measured current with respect to the simulated one is probably due to the drop of

critical current density caused by the heating. Since the circuit model is developed under the assumption that, regardless the losses produced during the quench, the ring temperature does not change, only the numerical results concerning a short period after the dissipative state is entered can be considered reliable. However the accurate simulation of the device dynamic during a short time interval after a fault event is crucial for the assessment of the impact of SCFCL on power systems.

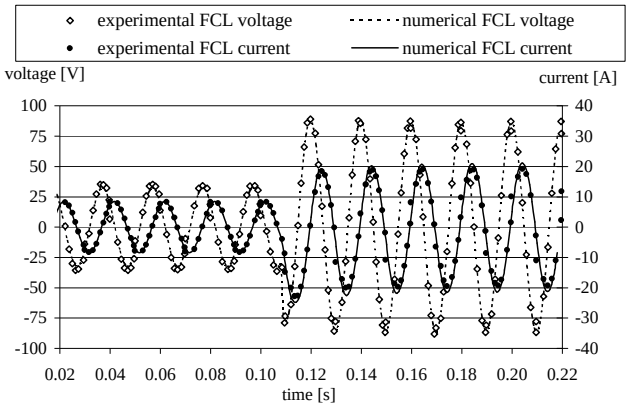

Figure 4.4.2: Current and voltage across the device during a fault. V_s = 70 V; T_{fault} = 110.4 ms.

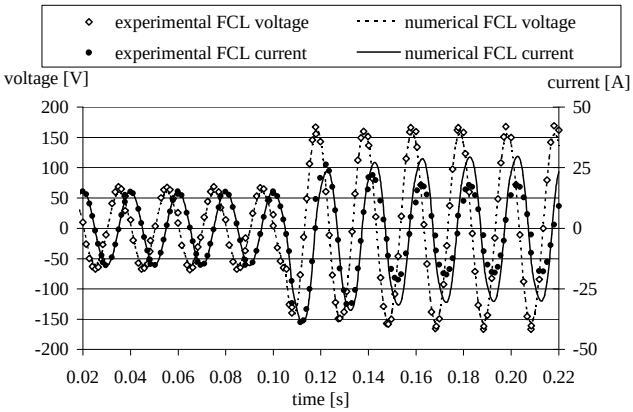

Figure 4.4.3: Current and voltage across the device during a fault. V_s = 130 V; T_{fault} =105.5 ms.